

Behavior of steel and carbon FRP-reinforced concrete-filled FRP tube columns under eccentric loads

R. Masmoudi¹, H.M. Mohamed², G. Benoit³

¹ Professor, University of Sherbrooke, Sherbrooke, QC, Canada

² Postdoctoral Fellow, University of Sherbrooke, Sherbrooke, QC, Canada

³ Master student, Lyon, France

ABSTRACT: This paper presents the performance of the reinforced concrete-filled FRP tubes (RCFFTs) columns under eccentric loads. The experimental program included two CFFT cylinders and ten RCFFT columns (152×912 mm). The main parameters examined include the type of internal reinforcement (steel and carbon FRP bars) and the eccentricity values. The load eccentricity-to-diameter (e/D) ratios were 0, 0.1, 0.2, 0.3 and 0.4. The test results indicated that the CFRP-CFFT columns successfully maintained the axial load carrying capacities and the induced moment under different eccentricities as compared with the counterpart steel-RCFFT columns. Also, the CFRP-specimens performed similarly to the specimens reinforced with steel bars up to the peak load in terms of stiffness, axial and lateral deformations. However, the strength and behavior of the test specimens were mainly affected by the eccentric loading. The compressive strength of CFFT columns was reduced by 42% to 75% with increasing the e/D ratio from 0.1 to 0.4.

1 INTRODUCTION

Concrete-filled fiber reinforced polymer (FRP) tubes (CFFTs) system is one of the most promising technique to protect the reinforced concrete structures from aggressive environmental conditions. In recent years, some applications of CFFT technique for different structural applications piles, columns, girders, bridge piers were accomplished (Fam et al. 2003). Several experimental and analytical investigations were conducted to study the behaviors of the CFFT columns, (Mohamed and Masmoudi 2010 and 2008; Mohamed et al. 2010; Mirmiran et al. 2001). However, most of the experimental investigations which have been conducted on CFFT columns were on unreinforced and under pure axial compression load. In fact, structural concrete columns under axial loads are exhibited to unintentional eccentric loads. This occurs for the edge and corner columns in the residential or office building and open garages. In addition, the designed axially loaded columns are subjected to the eccentricity due to unintentional load eccentricities, possible construction error, lateral deformation and buckling phenomenon. Also, there are many columns that are intended to carry eccentric loads. Therefore, it is important to understand the behavior of the CFFT columns under eccentric load. On the other hand, very few studies were conducted on FRP bars as compression reinforcement, (Wu 1999; Alsayed et al. 2000; Choo et al. 2006). This has made it necessary to create comprehensive studies needed to evaluate their potential use for CFFT technique under axial loads. In this study, 12 CFFT columns were tested under concentric and eccentric axial compression loads. The effects of the eccentricity-to-diameter (e/D) ratios and the type of

internal reinforcement on the behavior of CFFT columns are presented in terms of failure modes, ultimate load carrying capacities and load-deformation characteristics.

2 EXPERIMENTAL PROGRAM

2.1 Test Specimens

Table 1 summarizes different configurations of the tested specimens. The experimental program was carried out on twelve specimens, two CFFT cylinder and ten RCFFT columns. The twelve specimens were included through three series. The tested columns had a circular cross-section of 152 mm diameter. Series No. 1 had two replicas specimen with a total height 305 mm and without internal reinforcement. The objective of this particular series was to measure the ultimate capacity of short concrete column (the target failure mode of the column in this series was rupture in the FRP tube). This particular series intended to measure the mechanical characteristics (ultimate load, initial and tangent young's modulus) of the concrete confined with FRP tubes. Series No. 2 and 3 present RCFFT columns with a total height 912 mm, reinforced longitudinally with 6 steel or CFRP bars, respectively. The bars were distributed uniformly inside the cross section of the GFRP tube. The bars were fixed at the top and the bottom of the height using two steel stirrups of 3.2 mm diameter, to fix the bars during casting. The distance between the bars and the tubes was 8 mm. A concrete cover of 10 mm was provided between the ends of the longitudinal bars and the end surfaces to avoid the stress concentration at the bars area. In the specimens ID shown in the second column of Table 1, the numbers indicate the eccentricity (e) in mm and the letter S or C refers to the type of internal reinforcement, respectively, steel or CFRP rebars. The load eccentricity-to-diameter (e/D) ratios for the RCFFT columns were 0, 0.1, 0.2, 0.3 and 0.4.

2.2 Materials Properties

Glass-fiber reinforced polymer (GFRP) tubes were used as structural formwork for the CFFT specimens. The GFRP tubes were fabricated using filament winding technique; E-glass fiber and Epoxy resin were utilized for manufacturing these tubes. The tubes had a core diameter of 152 mm and a wall thickness of 2.65 mm (6 layers). The fiber orientations of the tubes were mainly in the hoop direction (± 60 degree with respect to the longitudinal axis). The split-disk test and coupon tensile test were performed according to ASTM D-2290-08 (ASTM 2008a) and ASTM D638-08 (ASTM 2008b) standard, respectively, on five specimens of the tubes. Figure 1 presents the axial tensile stress-strain response resulted from the coupon tests. In addition, Figure 2 shows the average stress-strain relationship for the split-disk test in the hoop direction. All specimens of this study were constructed using normal concrete strength. Concrete batch was supplied by ready mix concrete supplier. The 28-day average concrete compressive strength was found equal to 30 ± 0.6 .

Table 1. Specimens details and summary of test results

Series No.	Specimen ID	(e/D)	Rebar type	P_r (kN)	Δ_h (mm)	M_p (kN.m)	M_s (kN.m)	M_t (kN.m)	(f'_{cc}/f'_c)
1	CFFT Cyl	0	---	1572	----	---	---	---	2.90
	S-00	0	Steel	1480	7.30	---	---	---	2.30
2	S-15	0.1	Steel	825.0	31.00	13.14	12.38	25.51	1.04
	S-30	0.2	Steel	620.0	45.5	9.40	18.60	28.00	0.65
	S-45	0.3	Steel	466.0	60.00	6.87	20.97	27.84	0.36
	S-60	0.4	Steel	367.0	73.00	4.70	22.02	26.72	0.17
	C-00	0	CFRP	1343	3.20	---	---	---	2.20
3	C-15	0.1	CFRP	771.7	22.1	5.47	11.58	17.05	1.12

C-30	0.2	CFRP	614.5	43.46	8.28	18.44	26.71	0.82
C-45	0.3	CFRP	454.9	59.55	6.61	20.47	27.08	0.52
C-60	0.4	CFRP	375	75.32	5.74	22.50	28.24	0.37

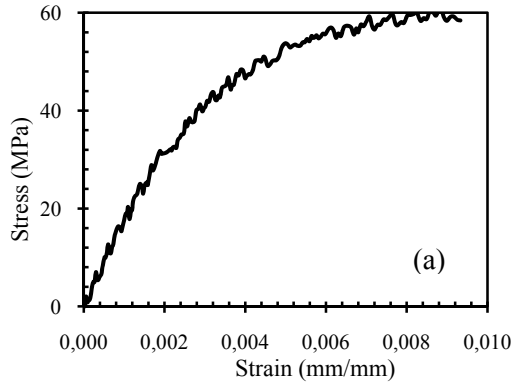


Figure 1. Stress-strain relationship for coupon tensile test

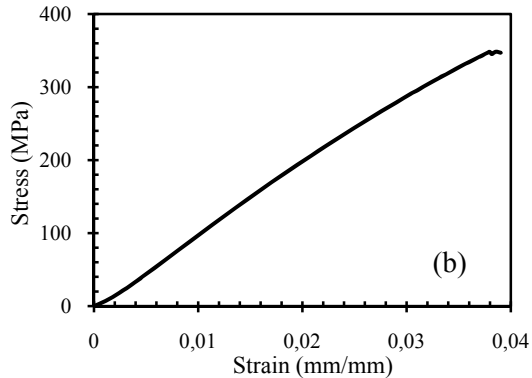


Figure 2. Stress-strain relationship for split-disk test.

Two types of reinforcing bars were used as longitudinal reinforcement for the CFFT columns; deformed steel bars No. 10 M (11.3 mm nominal diameter) and sand-coated carbon FRP (CFRP) bars No. 3 (9.52 mm nominal diameter). The mechanical properties of the steel bars were obtained from standard tests that were carried out according to ASTM A615/A615M-09, on five specimens for each type of the steel bars. The average values of the yield tensile strength, f_y was 462 with an ultimate tensile strength, f_{su} , 577 MPa. On the other hand, the CFRP bars were manufactured and developed by Pultrall Inc., Quebec, Canada. The bars were made of continuous fiber impregnated in vinylester resin with a fiber content of 73%, using the pultrusion process. The elastic modulus and ultimate tensile strength were 128 GPa and 1431 MPa with an ultimate tensile strain 1.2 ± 0.09 .

2.3 Instrumentation and Test Setup

Vertical and horizontal displacements of all specimens at their mid-height were monitored using linear variable displacement transducers (LVDTs). Strains in the longitudinal rebar reinforcement and FRP tubes were recorded using electric strain gauges, 6.0 mm in length. Two strain gauges were bonded to the mid-height of two longitudinal steel or CFRP bars, 180 degree apart. Two axial and two transversal strain gauges were installed on the FRP tubes on two opposite sides at the mid height of each column.

The concentric and eccentric loaded-CFFT specimens were tested under monotonically increasing axial compressive loading condition. The specimens were prepared before the test by a thin layer of the high strength Sulphur capping on the top and bottom surfaces to insure the uniform stress distribution during the test. For concentrically loaded CFFT columns, steel collars (4.0 mm thickness and 60.0 mm width) were attached to the ends of the specimens to prevent premature failure at these locations. For eccentrically loaded CFFT columns, the load was applied with specific eccentricities using specially designed two rigid steel end-cap and roller bearing assembly. The two rigid steel end-caps were designed and fabricated from high strength steel plates and semicircular section of thicknesses 30 mm and 5 mm, respectively. The steel plates and semicircular section were welded together with outward radiating stiffeners of thickness equal to 25 mm. The CFFT specimens were tested under four variable eccentric loads. Therefore, four lines holes were drilled at the top and bottom surfaces of the steel plate of the two caps at distance 15, 30, 45, 60 mm from the center of specimen's position to fix the roller steel rod. The caps sections were placed over the two ends of the CFFT specimens and clamped together 15 mm with high strength steel bolts. The specimens were tested using a 6,000 kN (1350 kips) capacity FORNEY machine, where the CFFT columns were setup vertically at the center of loading plates of the machine. Figure 3 show the rigid steel caps details and test setup for eccentrically and concentrically loaded CFFT columns.

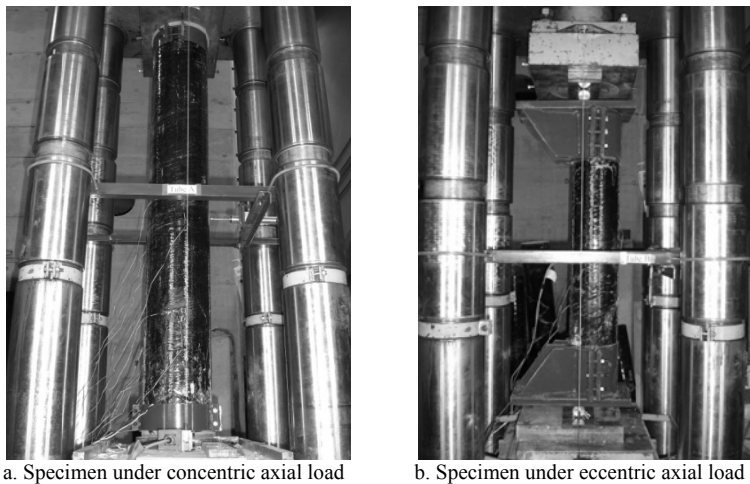


Figure 3. Test set up for concentric and eccentric axial load.

3 TEST RESULTS AND DISCUSSION

The test results indicated that the CFRP-RCFFT columns under eccentric loads behaved similarly to that of the counterpart reinforced with steel bars, in terms of load carrying capacities and deformations. However, the load carrying capacities of steel and CFRP-RCFFT columns were reduced due to the presence of the moment resulting from the applied load with eccentricity. Table 1 presents the peak loads (P_r), the primary moment (M_p) computed based on the initial (nominal) eccentricity, the secondary moment (M_s) caused by the lateral mid-height displacement at peak load, total moment at peak load (M_t) and the corresponding horizontal displacements at the mid-height of the columns (Δ_h). The table also includes concentrically loaded RCFFT columns of the same materials as a reference to emphasize the effect of load eccentricity on the behavior of the RCFFT columns. The total maximum moment M_t at mid-height, which is reported in Table 1 for all eccentrically loaded specimens, is composed of the

primary moment, based on the initial eccentricity, and the secondary moment due to the lateral deflection at failure at mid-height.

3.1 Ultimate Load Carrying Capacity and Eccentricity Effect

The ultimate capacity of all specimens was depicted versus the eccentricity to diameter (e/D) ratios values in Fig. 4. The figure shows that CFRP-RCFFT columns maintained approximately the same load carrying capacities of the counterparts steel-RCFFT specimens. The ultimate capacities of Specimens C00 and C15 were 9% and 6.5%, respectively, lower than that reinforced with steel bars S00 and S15. Increasing the e/D ratios from 0.2 to 0.3, the CFRP-RCFFT columns present insignificant decrease (less than 2%) in the ultimate load carrying capacities as compared with steel-RCFFT columns. However, the ultimate load of Specimens C60 with $e/D = 0.4$ was higher (2%) than that of Specimens S60. On the other hand, Fig. 4 confirms the fact that the ultimate load capacities of the CFFT specimens significantly decreased with increasing the eccentricity to diameter (e/D) ratios. For example, the decrease of the ultimate capacity of the Specimens S15, S30, S45 and S60 (with an eccentricity to diameter ratio changed from 0.1 to 0.4) compared to Specimens S00 was, respectively, 44%, 58%, 68% and 75%. The corresponding values for CFRP-RCFFT specimens were 42%, 54%, 66% and 72%, respectively, for Specimens C15, C30, C45 and C60. The confined concrete compressive strength to the unconfined concrete compressive strength ratio (f'_{cc}/f'_c) is given in Table 1. It was found that the gain in the confined strength decreased significantly with increasing the eccentricity-to-diameter ratios. The f'_{cc}/f'_c of steel-RCFFT columns decreased from 2.3 to 0.17 with increasing the e/D ratios from zero to 0.4, respectively. The corresponding values for CFRP-RCFFT columns were 2.2 to 0.37.

The experimental results were used to establish the interaction moment diagram. The load carrying capacity of eccentrically loaded columns was reduced due to the presence of the moment resulting from the applied load with initial eccentricity and lateral deformation. Therefore the mid-height moments induced in the specimen consist of two components, described by Equations below:

$$M_t = M_p + M_s \quad (1)$$

$$M_p = P_r \Delta_h \quad (2)$$

$$M_s = P_r e \quad (3)$$

Figure 5 shows the interaction moment diagram of steel and CFRP-RCFFT columns. The curve is of a similar shape to that which can be expected for a typical reinforced concrete column. It is clear that the maximum benefit of using GFRP tubes as a confinement mechanism occurs when the section subjected to pure axial loads. In addition, the figure reflects clearly the transition from tension to compression failure through the balanced point.

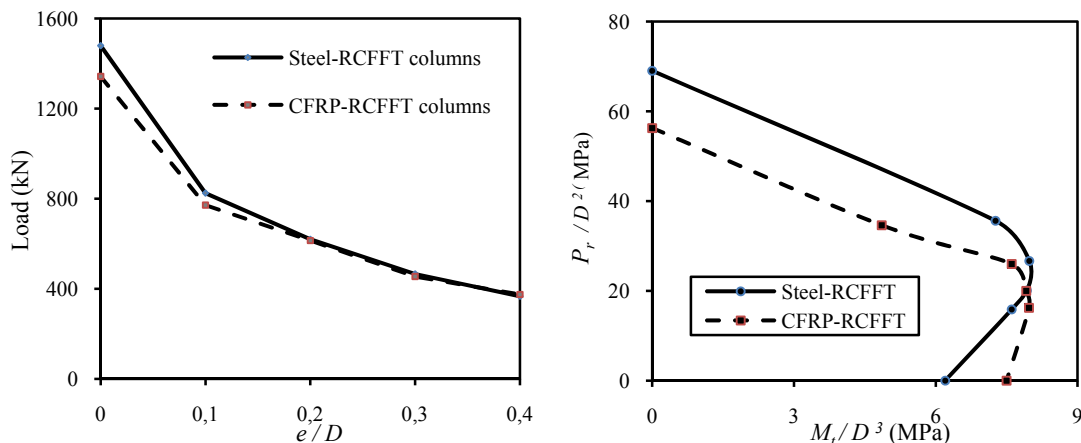


Figure 4. Load versus the eccentricity to diameter ratios Figure 5. Interaction moment diagram for RCFFT

Increasing axial load and moment, Specimens S45, S60, C45 and C60 failed mainly by tensile yielding of steel bars or rupture of CFRP bars and rupture of the FRP tube at the tension side. Specimens S30 and C30 present the balanced point on the curve. Above the balanced point, at which the curve reverses direction, the axial load increases and the total moment decreases which resulted from decreasing the eccentricity. Specimen S00 failed in compression, while Specimen S15 failed in compression and tension by crushing of the concrete at the compression side and rupture of the FRP tube in the axial direction at the tension side, respectively.

3.2 Axial and Lateral Deformations

The plotted results in Figure 6 represent the load–shortening relationships of the steel and CFRP-CFFT columns. It can be seen that the load–axial deformation curve of CFFT columns typically consisted of three stages. The first branch of these curves was almost linear and it defined the initial stiffness of the FRP-confined concrete columns. The load–shortening relationships of CFRP-RCFFT columns typically coincided with the counterpart that of steel-RCFFT columns. However, we found that the initial stiffness depended only on the eccentricity-to-diameter ratios regardless the type of longitudinal reinforcements (refer to Figure 6). For example, the decrease of the initial stiffness of the Specimens S15, S30, S45 and S60 (with an eccentricity to diameter ratio changed from 0.1 to 0.4) compared to Specimens S00 was, respectively, 65%, 73%, 82% and 85%. The corresponding values for CFRP-RCFFT specimens were 62%, 71%, 84% and 83%, respectively. The second stage of the curve is transition stage to the third branch of the load–axial deformation curve. With the propagation of the lateral cracks and because of the confining pressure, the load–deflection curve distinguished with a hardening region until the failure point, which is the third branch of the curve for concentrically loaded columns (S00 and C00). However, the third branch of the curve for eccentrically loaded columns presents a softening region with a significant decrease in the ultimate load. This reflects the fact that the confinement resulted from FRP tubes is less effective for eccentrically loaded columns that that of concentrically loaded columns. Figure 7 shows the load–lateral deformation relationships of the steel and CFRP-CFFT tested columns. For concentrically loaded columns, no lateral deformation was recorded up to 85% of the ultimate load due to axial loading, however for eccentrically loaded columns; the lateral displacement of the columns was significant indicating instability of the columns. The lateral deformation of the eccentrically columns increased gradually with the load increase up to the peak load. After that, the deformation increased progressively with a significant decrease in the load carrying capacities up to the complete instability of the column.

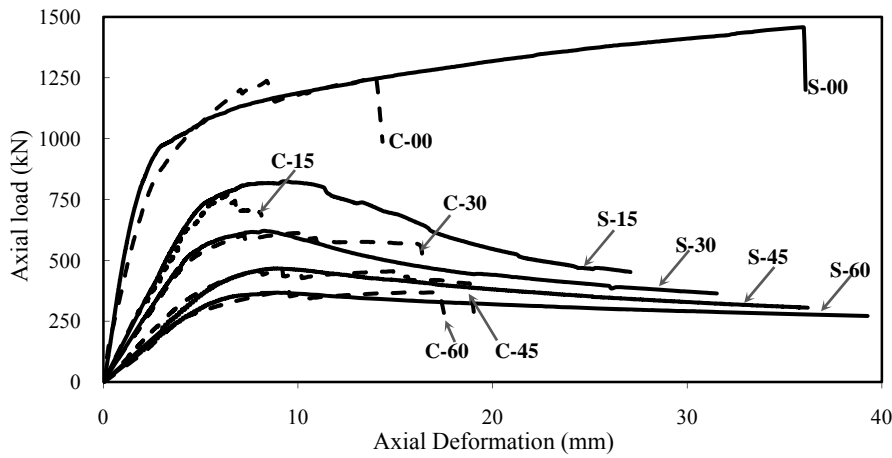


Figure 6. Load-shortening relationships for the steel and CFRP-RCCFT columns.

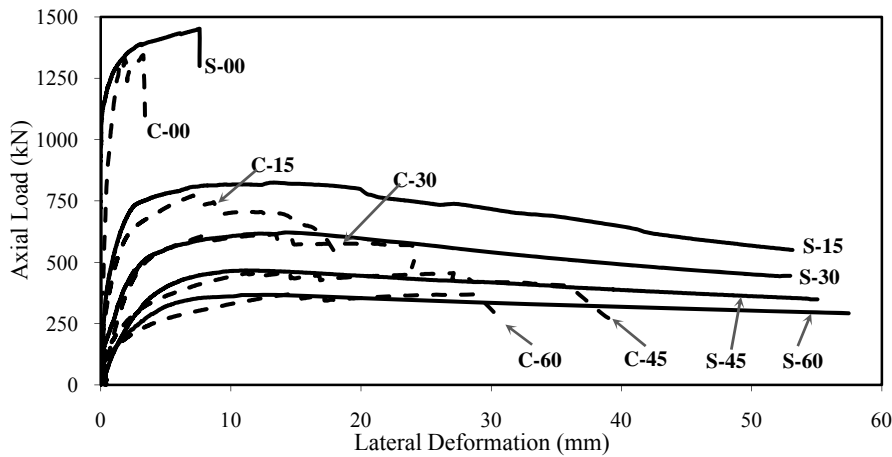


Figure 7. Load-lateral deformation relationships for the steel and CFRP-RCCFT columns.

3.3 Failure modes

The modes of failure of the CFFT specimens were characterized either by FRP tubes rupture (centrically CFFT columns) or columns instability (eccentrically loaded columns). Figure 8 shows the overview of the final failure modes for the concentrically and eccentrically loaded steel and CFRP-CFFT columns. The failure of steel-RCCFT columns was generally marked by a ductile failure as compared to those reinforced with CFRP bars. As the peak load was reached, horizontal flexural cracks propagated quickly through the tension side. Significant decrease in the ultimate load capacity was observed for all eccentrically specimens as compared with the ultimate load capacity of concentrically loaded CFFT columns. Excessive horizontal deformation at the mid height of the CFFT columns was observed beyond the peak load. The final failure mode for the eccentrically loaded CFFT columns was permanent with a single curvature in the direction of the tension side. Beyond the peak load, the failure was marked by the tensile rupture of the FRP tube at the tension side in the axial direction. On the other hand, minor local buckling in the compression side for the FRP tubes at the mid height was observed for Specimen S60 due to the increases in the lateral deformations.

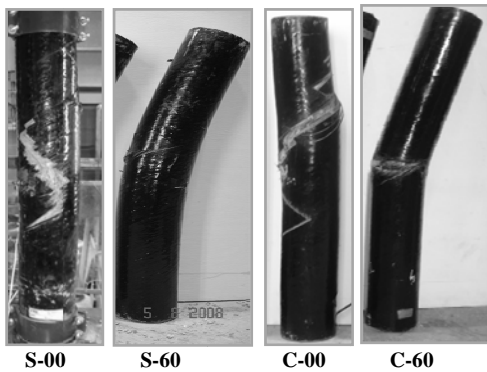


Figure 8. Failure modes of concentric and eccentric loaded steel and CFRP-RCFFT columns.

4 CONCLUSIONS

The main findings of this investigation can be summarized as follows:

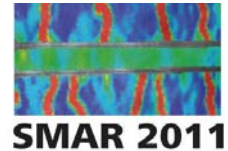
- The experimental investigation conducted in this study indicated that the CFRP-rebars can serve as an alternative to conventional steel reinforcement for concrete columns subjected to combined bending and axial loads.
- The results of the testing indicate that the CFRP-reinforced CFFT columns behaved similar to that reinforced with steel bars in terms of stiffness, strength, and axial and lateral deformation.
- The load carrying capacities of CFFT columns under load eccentricities, e/D ratios ranged from 0.10 to 0.4 were reduced by 42 to 75%, respectively, as compared to the that the same CFFT columns under concentric load.
- The axial and lateral deformations were increased progressively with increasing the eccentricity values.
- The failure mode of the CFFT columns is dependent on the type of loading. Rupture of the FRP tube in the hoop direction and local buckling of internal bars are the dominant in case of concentric loading. While the combination of tensile rupture of the FRP tubes and CFRP bars or steel yielding in the tension side with excessive axial and lateral deformations are the dominant in case of eccentric loading.

5 ACKNOWLEDGEMENTS

The research reported in this paper was partially sponsored by the Natural Sciences and Engineering Research Council of Canada (NSERC). The authors also acknowledge the contribution of the Canadian Foundation for Innovation (CFI) for the infrastructure used to conduct testing. Special thanks to the FRE Composites Inc, QC, Canada, for providing the FRP tubes.

6 REFERENCES

- Al-Sayed, S.H., Al-Salloum, Y.A., and Almusallam, T.H., 2000. Performance of glass fiber reinforced plastic bars as a reinforcing material for concrete structures. *Journal Composites Part B: Engineering*, Vol. 31, Issues 6-7, 555-567.
- ASTM. 2008a. Standard test method for apparent hoop tensile strength of plastic or reinforced plastic pipe by split disk method. D 2290-08, West Conshohocken, Pa.
- ASTM. 2008b. Standard test method for tensile properties of plastics. D638-08, West Conshohocken, Pa.



- ASTM. 2009. Standard specification for deformed and plain carbon steel bars for concrete reinforcement. A615/A615M-09, West Conshohocken, Pa.
- Choo, C. C., Harik, E. I., and Gesund, H. 2006. Strength of rectangular concrete columns reinforced with fiber-reinforced polymer bars. *ACI Structural Journal*, V. 103, 3: 452-459.
- Fam, A., Green, R., and Rizkalla, S. 2003. Field application of concrete-filled FRP tubes for marine piles. *ACI Special Publication*, SP-215-9, 161-180.
- Mirmiran, A., Shahawy, M., and Beitleman, T. 2001. Slenderness limit for hybrid FRP concrete columns. *Journal of Composites for Construction*, ASCE, Vol. 5, No.1, pp. 26-34.
- Mohamed, H., and Masmoudi, R. 2010. Axial load capacity of reinforced concrete-filled FRP tubes columns: experimental versus theoretical predictions. *Journal of Composites for Construction*, ASCE, Vol. 14, 2: 231-243.
- Mohamed, H., and Masmoudi, R. 2008. Compressive behaviour of reinforced concrete filled FRP tube. *ACI Special Publications (SP)*, SP-257-6, 91-109.
- Mohamed, H., Abdel Baky, H., and Masmoudi, R. 2010. Nonlinear stability analysis of concrete filled FRP-tubes columns: experimental and theoretical investigation. *ACI Structural Journal*, 2010, impress.
- Wu, W.P. 1990. Thermomechanical properties of fibre reinforced plastic (FRP) bars. West Virginia, University, Morgantown, WV., PhD dissertation.